Int. J. Multiphase Flow Vol. 15, No. 3, pp. 371–384, 1989
Printed in Great Britain.

0301-9322/89 $3.00 + 0.00

PERIODIC AND SOLITARY WAVES ON THIN, HORIZONTAL, GAS-SHEARED LIQUID FILMS

L. A. JURMAN, K. BRUNO and M. J. MCCREADY
Department of Chemical Engineering, University of Notre Dame, Notre Dame, IN 46556, U.S.A.

(*Received* 6 *July* 1988; *in revised form* 23 *November* 1988)

Abstract—Measurements of wavelengths and speeds of periodic waves which occur at the interface of thin, horizontal, liquid films sheared by a cocurrent gas flow are compared with predictions of linear theory. In general, linear predictions accurately match the data near the point of neutral stability but begin to deviate as the gas velocity increases. The behavior away from neutral stability is explained by the examination of the dynamical system associated with steady solutions to a nonlinear wave equation based on boundary-layer approximations. Periodic waves are seen to occur in the neighborhood of the Hopf curve which serves as a boundary between periodic waves and a flat film. Solitary waves (which correspond under some circumstances to disturbance or roll waves) are observed to lie in another region of parameter space at gas velocities well above neutral stability. These results suggest that a complete nonlinear analysis of the boundary-layer (or associated wave) equations would be useful for predicting amplitudes and speeds for periodic waves and the region of occurrence for solitary waves.

Key Words: gas–liquid flows, solitary waves, wave equation

1. INTRODUCTION

A characteristic common to all annular flows is the wavy gas–liquid interface. Waves exert a significant influence on the flow fields of both liquid and gas by causing fluctuations in the wall shear stress (and consequently on heat or mass transfer rates). They also affect the rate of atomization from the film and influence pressure drop because of roughening of the interface. Quite clearly, a complete understanding of the annular flow regime will not occur until the interfacial wave behavior is characterized.

Because of their obvious importance, waves on thin films have been the subject of numerous studies. Examples of studies of waves on freely falling films include those of Telles & Dukler (1970), Chu & Dukler (1974), Lin (1974), Nakaya (1975), Pumir *et al.* (1983), Alekseenko *et al.* (1985), Chang (1986a,b), Chen & Chang (1986) and Barrdahl (1986). Studies of waves on vertical films in the presence of a gas flow have been undertaken by Webb & Hewitt (1975), Henstock & Hanratty (1976), Nencini & Andreussi (1982) and Martin & Azzopardi (1985). For the case of freely falling films, the qualitative wave behavior is relatively well understood. Chang (1986b) has shown that for small liquid Reynolds numbers (< 10), accurate quantitative predictions of behavior can be obtained directly from Navier–Stokes equations simplified using perturbation arguments. However for higher liquid Reynolds numbers, the problem is much more difficult because the surface curvature is not small. The studies of Brauner & Maron (1983) and Maron *et al.* (1985) indicate that if the wave is broken into several separate regions, it is possible to describe its behavior. Wasden & Dukler (1987) were able to successfully describe speeds of waves on falling films using finite difference solutions to the Navier–Stokes equations when the shape of the interface was known from measurements.

Horizontal gas–liquid flows where the film is thin have also been studied but have not received the extensive attention accorded to falling films. Researches include Hanratty & Engen (1957), Hanratty & Hershman (1961), Cohen & Hanratty (1965), Craik (1966), Hanratty (1983) and Fukano *et al.* (1985). All of the theoretical analyses have been based on linear theories which have been shown to be capable of predicting wave speeds and conditions of neutral stability. Jurman & McCready (1989) used boundary-layer arguments to derive a weakly nonlinear wave equation which was shown to correctly match the equations of Hanratty (1983) in the linear limit. However, this equation has not been analyzed as to its ability to predict behavior when nonlinear effects are expected to be important.

Several issues need to be addressed to expand the present understanding of waves which occur on highly-sheared horizontal films. A theoretical approach which is based on the Navier–Stokes equations, but is sufficiently simple to allow examination of qualitative behavior of the solutions, is needed. It is necessary to verify, by comparison to experiments, that the approach is correct. A third need is to identify the processes which are occurring in these flows which lead to wave behavior. Specifically, what is the origin of the various wave types and for nonperiodic waves, what controls the number which occur.

In this study, waves occurring on thin liquid films, highly sheared by a gas flow, are investigated using experimental and theoretical techniques. For theoretical purposes, waves will be considered as individual, traveling forms because their wavelengths will be much longer than the film thickness; this precludes significant interaction between different waves. Surface tracings of waves are presented to display their qualitative behavior; measurements of speeds and wavelengths are used to evaluate the quantitative predictions of the equation derived by Jurman & McCready (1989). In addition, the qualitative behavior of steady solutions to this equation are examined. In the discussion, important outstanding questions about wave behavior are addressed.

2. EXPERIMENTAL METHOD

The flow system used in this study is a horizontal, rectangular flow channel with dimensions 2.54 cm high, 0.30 m wide and 9 m long through which gas and liquid flow concurrently (figure 1). Waves are measured with parallel wire conductance probes using techniques described by Henstock (1977) and McCready (1986). The probes used in this study are located approx. 6 m from the channel inlet. Filtered air is used as the gas and glycerin–water solutions having viscosities in the range of 10–20 cP are used as the liquid. The viscosity range was chosen because all events occur more slowly than with water and the waves tend to be two-dimensional. As a consequence, it is much easier to examine the waves experimentally and also to find conditions which should agree almost exactly with theory. Data were taken over a wide range of flow conditions and are presented here in the form of surface tracings, frequency spectra obtained from Fourier analysis of the surface height time series and average wave speeds obtained from cross-spectra using two probes separated by 0.55 cm.

Results and observations

Typical qualitative behavior for waves is displayed by the surface tracings in figure 2 where the liquid film thickness, m, is plotted vs time. Three conditions of increasing Re_G are shown. At the lowest value of $Re_G = 9850$, the waves observed are uniform and periodic. These waves form within the first 30–50 cm of the channel inlet and propagate with little change of shape. It is noted that these waves are highly two-dimensional with individual crests spanning almost the entire channel width. In figure 2(a), the film thickness is approx. 3 mm and the wavelength (obtained from photographs) is about 2 cm. If the gas velocity is increased while the liquid flow rate (and consequently Re_L) is held constant, the average film thickness decreases and a dramatic change occurs in the nature of the waves. Solitary waves appear and become dominant with essentially no periodic waves being present. The solitary waves form within a short distance from the beginning of the channel and propagate with little change of shape. Visual observations indicate that the width of the wave crests for these conditions is typically 8–12 cm. Surface tracings taken at higher Re_L exhibit similar behavior.

Also of interest are the corresponding wave amplitude–frequency spectra for these conditions which are shown in figure 3. As expected, the nearly sinusoidal periodic waves produce a clear peak that occurs at about 10 Hz. However, the shape of the solitary waves cannot be represented by only a few Fourier components, resulting in spectrum which is rather broad and flat.

It can be seen in the tracings of figure 2, that the waves at a given flow condition are quite uniform with respect to wavelength, shape and amplitude. In addition, because typical wavelengths are much larger than the film thickness [the conditions of figure 2(a) are typical for a range of films at low Re_L], only very weak interactions between different waves will occur. Therefore, it should be possible to describe the shape, amplitude and celerity of these waves with a nonlinear evolution equation using an analysis which focuses on the behavior of individual waves.

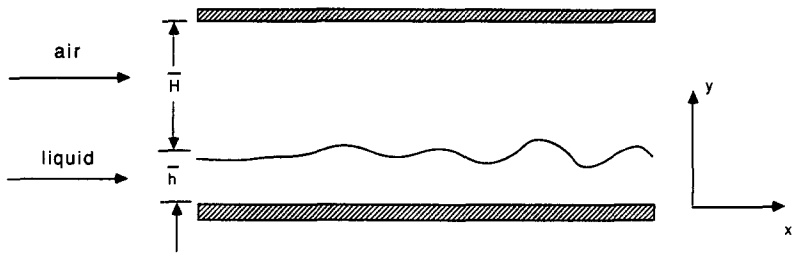

Figure 1. Gas–liquid flow system.

3. THEORY

For $Re_L \leqslant 20$ (based on the film thickness), the waves which appear as the result of a shearing turbulent gas flow will generally have wavelengths which are much longer than the film thickness. Consequently, theoretical analyses can be based on boundary-layer arguments. Starting with the boundary-layer equations, Jurman & McCready (1989) showed that for two-dimensional waves on thin liquid films sheared by gas flows, the surface height should be described by the equation

$$\left(\frac{\partial}{\partial t}+c_1\frac{\partial}{\partial x}\right)\left(\frac{\partial}{\partial t}+c_2\frac{\partial}{\partial x}\right)h+\frac{3}{\alpha\,Re_L}\left(\frac{\partial}{\partial t}+c_0\frac{\partial}{\partial x}\right)h-\hat{p}_{si}h_{xxx}+\alpha^2 We h_{xxxx}$$
$$=-\frac{3}{\alpha}\left(\frac{2}{Re_L}+2\hat{\tau}_{sr}-\frac{4\alpha}{3}\frac{d\bar{p}_s}{dx}\right)h\frac{\partial h}{\partial x}+2(\bar{\Gamma}-1)\frac{\partial}{\partial t}\left(h\frac{\partial h}{\partial t}\right)$$
$$-3\left(\frac{\hat{\tau}_{si}}{\alpha}-\hat{p}_{sr}-\gamma\right)\frac{\partial}{\partial x}(h\,h_x)+3\hat{p}_{si}\frac{\partial}{\partial x}(h\,h_{xx}), \qquad [1]$$

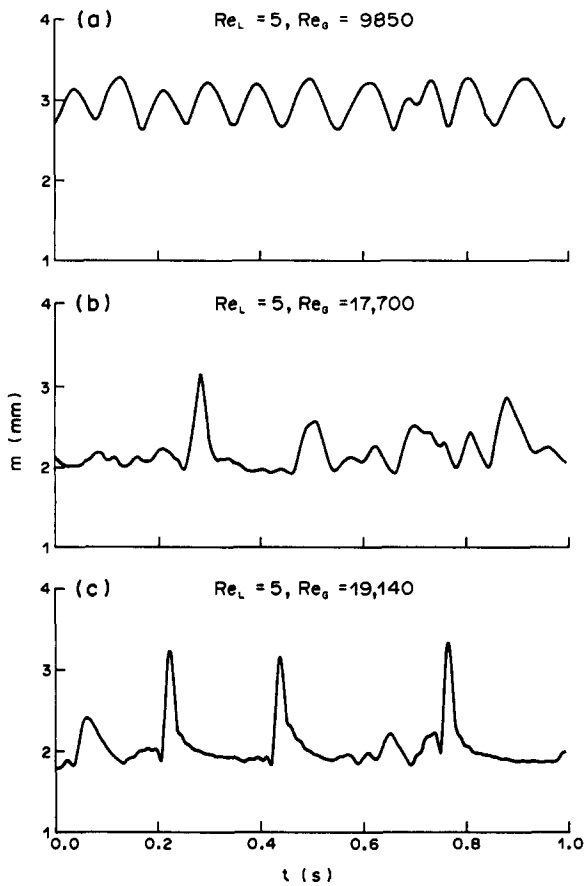

Figure 2. Surface tracings at $Re_L = 5$ as a function of increasing gas velocity, $\mu \sim 12$ cP.

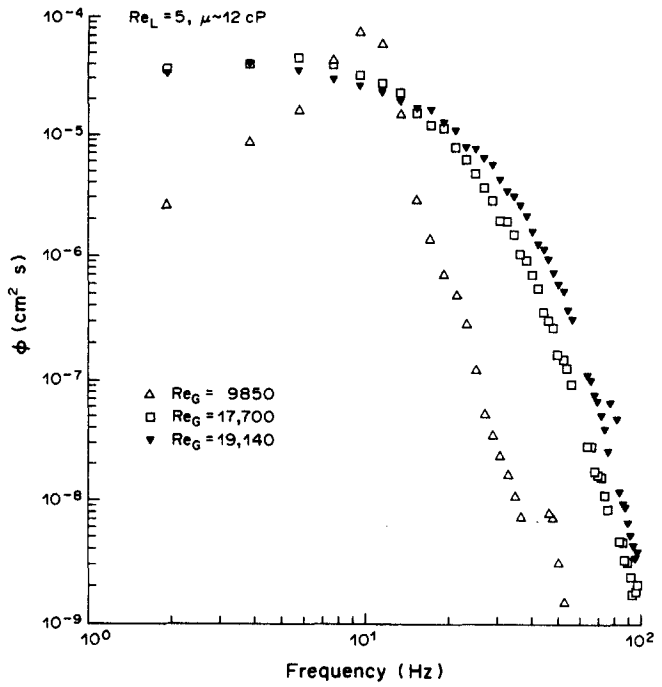

Figure 3. Frequency spectra at $Re_L = 5$ as a function of increasing gas velocity.

where

$$c_0 = 2 + \frac{Re_L \hat{\tau}_{sr}}{2} - \frac{\alpha\, Re_L}{3}\frac{d\bar{p}_s}{dx} \qquad [2]$$

and

$$c_{1,2} = \bar{\Gamma} \pm \sqrt{(\bar{\Gamma}^2 - \Gamma) - \frac{3\tau_{si}}{2\alpha} + \hat{p}_{sr} + \gamma}. \qquad [3]$$

In these equations, c_0 is the approximate kinetic wave speed, $c_{1,2}$ are approximate dynamic wave speeds, h is the surface height deviation from the average film thickness, α is the wavenumber made dimensionless with the average film height,† x is the flow direction, γ is an inverse Froude number, We is a Weber number and Re_L is the liquid Reynolds number. To derive an equation in terms of h, the boundary-layer equations are integrated over the film thickness. As a consequence, it is necessary to know the velocity profile. In their derivation, Jurman & McCready (1989) assumed that the profiles would be self-similar and described by Γ, the integral over the film thickness of the velocity squared. Another important assumption in this derivation is that the effect of the gas flow can be described through boundary conditions on pressure and shear stress which are written as components in-phase with the wave height ($\hat{p}_{sr}$ and $\hat{\tau}_{sr}$) and with the wave slope ($\hat{p}_{si}$ and $\hat{\tau}_{si}$), as has been done previously by Cohen & Hanratty (1965) and Craik (1966). Because this equation includes nonlinearities up to second order, it can be expected to provide information about small (but finite) amplitude waves. In the present case, where the liquid viscosity is >10 cP, this should include the entire periodic wave region. Linear analyses, such as Orr–Sommerfeld equations, can provide no information (e.g. amplitude) about finite amplitude waves.

(a) Linear analysis

Jurman & McCready (1989) examined the behavior of the linear stability predictions of [1]. They found that [1] gives predictions identical to the boundary-layer equations from which it is derived and in its high wavenumber limit, matches the predictions of an Orr–Sommerfeld equation (which

†Variables, with the exception of x, are made dimensionless using the average film height, $\bar{h}$, as a length scale and $\bar{h}/\bar{u}$ (the average film velocity) as a time scale.

is expected to be valid for higher wavenumber waves). In addition, if the variables that describe the behavior of the gas phase are obtained from the relations for turbulent flow over a solid wavy surface given by Abrams (1984) and Abrams & Hanratty (1985), then the wavelength of the maximum in the growth rate is shown to agree well for a Re_G not far above the neutral stability point. It if of interest to compare the predictions of [1] with data for wavelength and speeds over a wide range of conditions to test its applicability. If [1] is linearized about the flat film in terms of a small amplitude, periodic traveling disturbance the result is

$$c^2+\left(i\frac{3}{\alpha\,\mathrm{Re_L}}-2\bar{\Gamma}\right)c+\left(\bar{\Gamma}+\frac{3\hat{\tau}_{si}}{2\alpha}-\hat{p}_{sr}-\gamma-\alpha^2\,\mathrm{We}\right)$$
$$-i\frac{3}{\alpha\,\mathrm{Re_L}}\left(2+\frac{\mathrm{Re_L}\hat{\tau}_{sr}}{2}-\frac{\alpha\,\mathrm{Re_L}}{3}\frac{d\bar{p}_s}{dx}+\frac{\alpha\,\mathrm{Re_L}}{3}\hat{p}_{si}\right)=0, \quad [4]$$

where c is the complex wave velocity. Examination of [4] reveals that no maximum exists for predicted growth rates in the high wavenumber limit and that for many conditions, all waves with wavenumbers greater than a certain value are predicted to be unstable. This behavior is unrealistic physically and results because the long-wavelength assumptions break down. To describe the linear behavior of waves with higher wavenumbers (shorter wavelengths), the Orr–Sommerfeld analysis given by Hanratty (1983), which is also about the flat film state, will be used. The secular equation for the complex velocity in this case is

$$\alpha(u_s-c)^2\coth(\alpha\bar{h})-\left(\frac{d\bar{u}}{dy}\right)_s(u_s-c)$$
$$=G+\frac{i\hat{\tau}_s}{\rho_L}\left[\coth(\alpha\bar{h})-\frac{1}{\alpha(u_s-c)}\left(\frac{d\bar{u}}{dy}\right)_s\right]-(\alpha\bar{h})^{1/2}\left(-i\frac{\bar{h}c}{\nu_L}\right)^{-1/2}\{\alpha(u_s-c)^2[1-\coth^2(\alpha\bar{h})]\}$$
$$+4i(\alpha\bar{h})\left[\frac{\bar{h}(\bar{u}_s-c)}{\nu_L}\right]^{-1}\alpha(u_s-c)^2\left[\coth(\alpha\bar{h})-\frac{1}{\alpha(u_s-c)}\left(\frac{d\bar{u}}{dy}\right)_s\right], \quad [5]$$

where

$$G=\frac{\hat{P}_s}{\rho_L}+\frac{\sigma\alpha^2}{\rho_L}+g. \quad [6]$$

Predictions of [4] and [5] for wave speeds at several sets of conditions are shown in figure 4. In figure 5, growth rates for corresponding conditions are shown. Because long-wavelength approximations are used to derive [1], its linear predictions are expected to be valid up to about $\alpha\cong 1$ (where $m/\lambda\cong 0.15$). As noted by Hanratty (1983), the Orr–Sommerfeld analysis will not be valid for small α because the term $\alpha(\bar{h}c_r/\nu_L)$ will not be sufficiently large. As a result of this, the growth rates predicted by the Orr–Sommerfeld equation are quadratic in α and do not display the more complex behavior (i.e. inflexion points) which is contained in the predictions of [4]. It is noted that growth rates obtained from [5] do exhibit maxima, as expected on physical grounds.

It is desirable to be able to predict the dominant wavelength as it is the most fundamental wave property. Linear analyses suggest that the mode which is fastest growing will appear. However, once waves have evolved into a stable form, other behavior might occur. Figure 6 shows a comparison of both predicted and measured wavenumbers for three sets of data where periodic waves are observed at $Re_L=4$, 8 and 12 over a range of Re_G. Also shown are values of the wavenumber which correspond to Hopf bifurcations. The equation which defines the Hopf wavenumber will be derived below. The Hopf wavenumber is of interest because it corresponds to the longest wavelength mode which is linearly unstable. It is seen that for $Re_L=4$ and 8 the growth rate maximum from [5] corresponds closely to the measured waves for low Re_G but begins to deviate at higher Re_G. For higher Re_G, the stable periodic waves have wavelengths which are somewhat longer than the predictions of linear stability theory suggest. Apparently, as the amplitude of waves increase, a longer wavelength provides a more stable shape. For $Re_L=12$, the

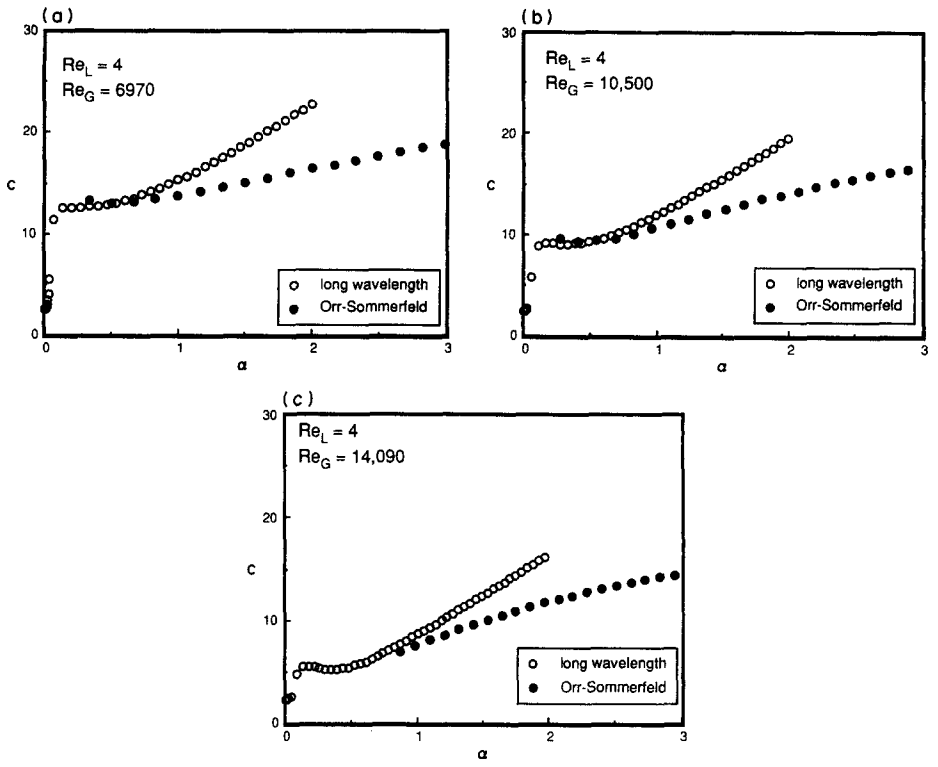

Figure 4. Comparison of wave speeds predicted by long-wavelength and Orr–Sommerfeld equations.

data fall consistently below the linear prediction. It is interesting to note that for all of the data presented here, the wavelengths of the dominant waves have values bounded by the fastest growing wave (minimum wavelength) and the Hopf bifurcation (maximum wavelength).

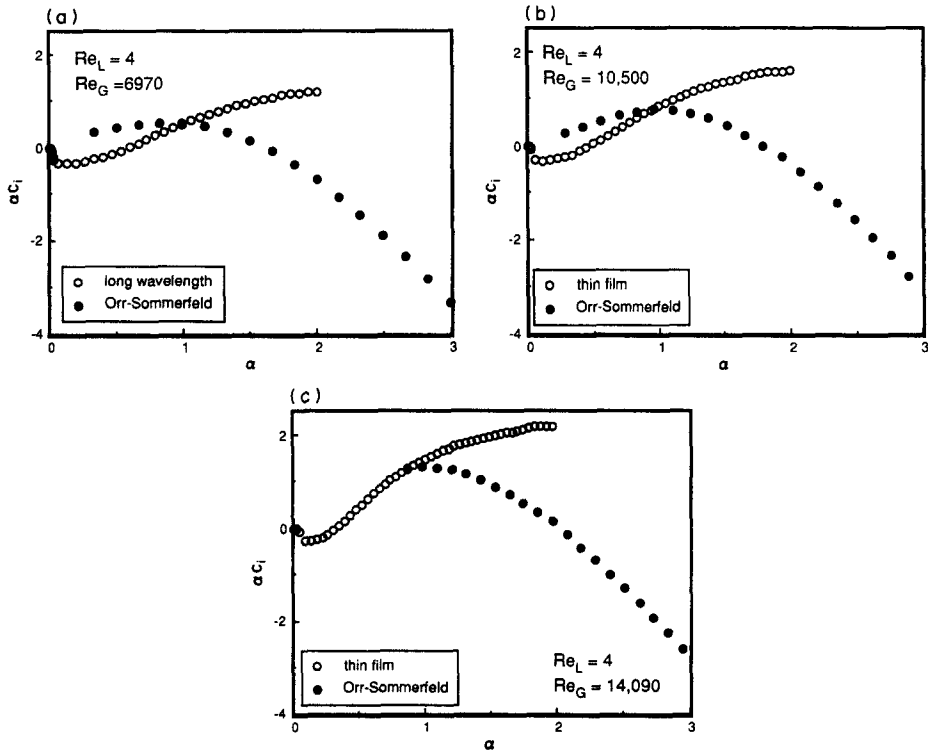

Figure 5. Comparison of growth rates predicted by long-wavelength and Orr–Sommerfeld equations.

In figure 7, a comparison is shown of measured values of the average wave speed with the predictions of [4] or [5] depending upon the value of α. For $Re_L = 4$ and 8, the agreement is excellent indicating that, apparently, the slope of the waves is not large enough to cause large deviations in the speed from linear predictions. For $Re_L = 12$ the measured wave speeds are consistently above the predictions with the exception of the first data point. It is not clear if this is due to nonlinear effects or a consistent error in the calculation. A small inaccuracy in the measured average film heights could cause calculation errors of the magnitude of the deviations which occur in this figure.

The data for periodic waves support the linear predictions of [4] and [5] as well as the use of the Abrams data and correlations for predicting the effect of the turbulent gas flow on the liquid. However, it is clear that steady waves cannot be explained by purely linear analyses. Figure 6 indicates that wavelengths for periodic waves are not accurately predicted by linear theory. In addition, experiments shown in figure 2 demonstrate that as the gas velocity is increased, wave behavior changes rather dramatically and steady solitary waves exist for higher gas velocities (these are expected to be prevalent for annular flow conditions). It is therefore desirable to develop a theoretical formulation which is capable of predicting the complete qualitative behavior which occurs. Solitary waves are highly nonlinear and even their initial formation cannot be described by linear analyses as they do not result directly from small-amplitude disturbances on the film. It is of interest to examine [1] with nonlinear terms included to see if it is capable of predicting, at least qualitatively, the behavior which leads to the appearance of solitary waves.

(b) Analysis of steady solutions to the wave equation

As the data indicate that both periodic and solitary waves appear as steady traveling forms, it is convenient to look at steady solutions to [1]. If this is done, techniques of nonlinear analysis which have been described by Guckenheimer & Holmes (1983) and Carr (1981), and used for the study of waves by Hwang & Chang (1987), can be applied to provide important information about the behavior of solutions to [1] in specific regions of parameter space without requiring complete numerical solutions. The development given here will be limited to initial formulation of the problem and identification of some aspects of the qualitative behavior.

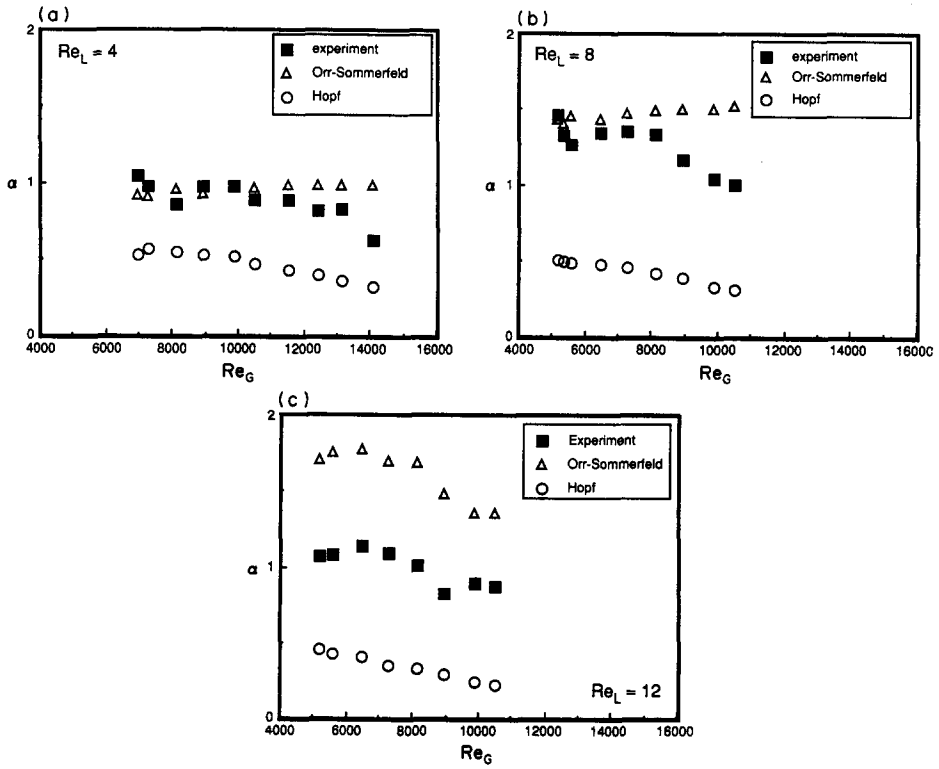

Figure 6. Comparison of predicted and experimental wavenumbers.

Following Hwang & Chang (1987), [1] can be transformed into a moving coordinate system by using the variable transformation, $\xi = x - c_r t$ where c_r is an unspecified wave speed. When this is done, the time derivatives $\partial/\partial t$ become $-c_r \partial/\partial x$, leading to

$$(c_r^2 - c_r(c_1 + c_2) + c_1 c_2)h_{\xi\xi} + A_0(c_0 - c_r)h_\xi + A_2 h_{\xi\xi\xi} + A_3 h_{\xi\xi\xi\xi} + B_1 h h_\xi + (B_2 + B_4 c_r^2)(h h_\xi)_\xi + B_3(h h_{\xi\xi})_\xi = 0, \quad [7]$$

where

$$A_0 = \frac{3}{\alpha\, \mathrm{Re}_L},$$

$$A_2 = -\hat{p}_{si},$$

$$A_3 = \alpha^2\, \mathrm{We},$$

$$B_1 = \frac{3}{\alpha}\left(\frac{2}{\mathrm{Re}_L} + 2\hat{\tau}_{sr} - \frac{4\alpha}{3}\frac{d\bar{p}_s}{dx}\right),$$

$$B_2 = 3\left(\frac{\hat{\tau}_{si}}{\alpha} - \hat{p}_{sr} - \gamma\right),$$

$$B_3 = -3\hat{p}_{si}$$

and

$$B_4 = -2(\bar{\Gamma} - 1).$$

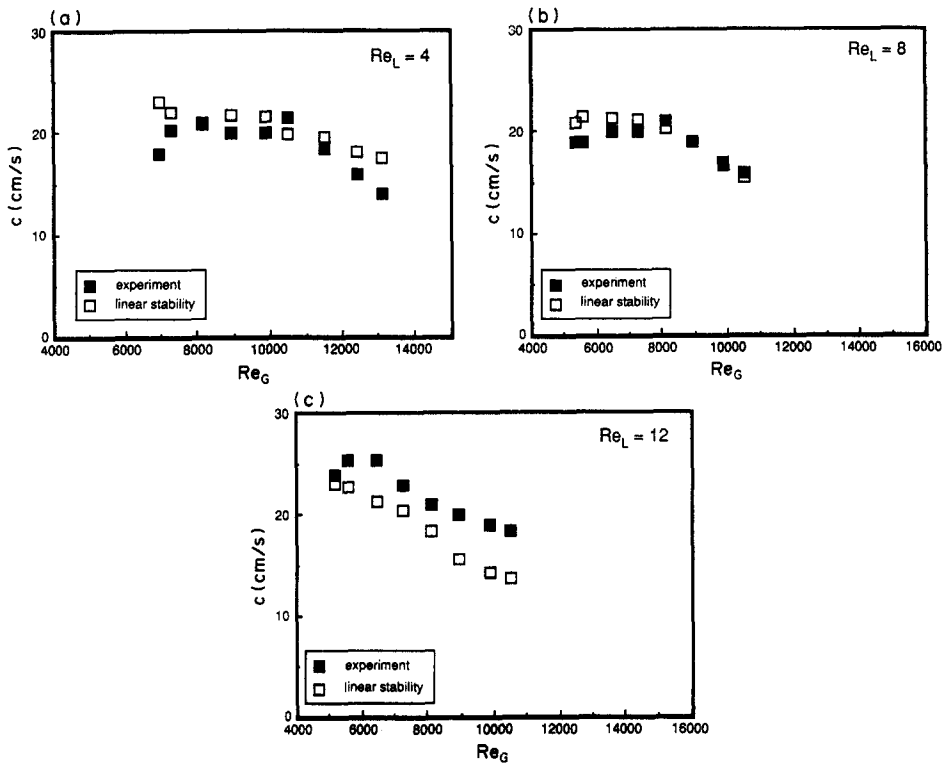

Figure 7. Comparison of predicted and experimental wave speeds.

Equation [7] is exactly integrable. In order for a flat film to be a solution, the integration constant must be zero. When [7] is integrated and the resulting equation is transformed into a system of first-order equations the result is

$$\mathbf{u}' = \begin{bmatrix} 0 & 1 & 0 \\ 0 & 0 & 1 \\ -D_0 & -D_1 & -D_2 \end{bmatrix} \begin{pmatrix} u_1 \\ u_2 \\ u_3 \end{pmatrix} + \begin{pmatrix} 0 \\ 0 \\ -E_1 u_1^2 - E_2 u_1 u_2 - E_3 u_1 u_3 \end{pmatrix}, \qquad [8]$$

where the prime denotes differentiation with respect to ξ, the vector $\mathbf{u}$ represents h, h' and h'' [$\mathbf{u} = (h, h', h'')^T$]. The coefficients are given as

$$D_0 = \frac{A_0}{A_3}(c_0 - c_r),$$

$$D_1 = \frac{(c_r^2 - c_r(c_1 + c_2) + c_1 c_2}{A_3},$$

$$D_2 = \frac{A_2}{A_3},$$

$$E_1 = \frac{B_1}{2A_3},$$

$$E_2 = \frac{(B_2 + B_4 c_r^2)}{A_3}$$

and

$$E_3 = \frac{B_3}{A_3}.$$

As is common for wave equations, system [8] possesses two fixed points which are always solutions. (Fixed points are stationary solutions which do not change or oscillate in time.) One is the flat film solution and the other is a shock solution. These are given by

$$\mathbf{u}^0 = \begin{pmatrix} 0 \\ 0 \\ 0 \end{pmatrix} \quad \text{and} \quad \mathbf{u}^1 = \begin{bmatrix} \dfrac{-D_0}{E_1} \\ 0 \\ 0 \end{bmatrix}. \qquad [9]$$

The amplitude of shock (given in $\mathbf{u}^1$) is dependent upon its speed which appears in D_0. The region of parameter space on which $D_0 = 0$ is where the two fixed points coalesce and is called a simple bifurcation.

To determine the generic qualitative behavior predicted by [8], the Jacobian matrix may be computed around the two fixed points. Defining

$$g_1 = u_2, \quad g_2 = u_3$$

and

$$g_3 = u_3' = -D_0 u_1 - D_1 u_2 - D_2 u_3 - E_1 u_1^2 - E_2 u_1 u_2 - E_3 u_1 u_3,$$

then

$$\mathbf{Dg} = \begin{bmatrix} 0 & 1 & 0 \\ 0 & 0 & 1 \\ \dfrac{\partial g_3}{\partial u_1} & \dfrac{\partial g_3}{\partial u_2} & \dfrac{\partial g_3}{\partial u_3} \end{bmatrix}, \qquad [10]$$

with

$$\frac{\partial g_3}{\partial u_1} = -D_0 - 2E_1 u_1 - E_2 u_2 - E_3 u_3,$$

$$\frac{\partial g_3}{\partial u_2} = -D_1 - E_2 u_1$$

and

$$\frac{\partial g_3}{\partial u_3} = -D_2 - E_3 u_1.$$

For $\mathbf{u}^0$ this gives

$$\mathbf{Dg}^0 = \begin{pmatrix} 0 & 1 & 0 \\ 0 & 0 & 1 \\ -D_0 & -D_1 & -D_2 \end{pmatrix} \qquad [11]$$

and for $\mathbf{u}^1$

$$\mathbf{Dg}^1 = \begin{bmatrix} 0 & 1 & 0 \\ 0 & 0 & 1 \\ D_0 & -D_1 + \dfrac{D_0 E_2}{E_1} & -D_2 + \dfrac{E_3 D_0}{E_1} \end{bmatrix}. \qquad [12]$$

Examination of the characteristic equation for [11] indicates that if D_0 and D_1 are simultaneously equal to zero, then two of the eigenvalues will be zero leading to a so-called "double zero" singularity. Singularities are of interest because they often serve as organizing centers in phase space. The analysis of Carr (1981) indicates that both a simple bifurcation and Hopf bifurcations can emanate from the present singularity. As mentioned above, a simple bifurcation will exist for conditions when $D_0 = 0$, which results in one of the eigenvalues of [11] being zero. Hopf bifurcations will occur along a curve, where $D_1 = D_0/D_2$. A Hopf bifurcation occurs in situations where a pair of purely imaginary eigenvalues, suggesting the existence of periodic oscillating solutions (limit cycles), occur for the Jacobian. For the present system, the Hopf curve is the locus of points at which the wave growth rate obtained from linear stability is exactly zero; waves with wavelengths shorter than the one at the Hopf point are predicted to be linearly unstable. Similar behavior will occur around the second fixed point, which shares the identical double zero point.

A general analysis of a double zero point by Carr (1981) indicates limit cycles (which correspond to periodic waves) can be expected in the vicinity of the Hopf and that homoclinic orbits (which correspond to solitary waves) are expected as well. In addition, the bifurcation curves, either Hopf or simple, are expected to serve as boundaries of qualitative wave behavior—separating, for example, regions where no steady solutions exist from periodic waves. In figure 8, the simple and Hopf bifurcation curves are plotted for $Re_L = 4$, 8 and 12 along with the wave speed of the dominant periodic waves. Several interesting features should be noted. The double zero is a function of Re_L and will occur at the point at which the speeds for Hopf curve and the simple curve become equal. It can be seen that periodic waves occur in the vicinity of Hopf curve and in all cases (within experimental error) have speeds which lie above the Hopf. For the present system, the Hopf curve is apparently acting as a boundary between periodic waves and a flat film; steady waves cannot exist with wave speeds less than the Hopf curve. For comparison, the wave speeds of the fastest growing modes using [5] are also shown. For the two lower Re_L values, approximate upper bounds on the wave speeds are given by the predictions of the peak speeds. However, the Orr–Sommerfeld peak growth rate is not expected to serve as a boundary between wave types and the data for $Re_L = 12$ indicate that it does not serve as any generic boundary for the present problem.

In figure 9, wave speed data including both periodic and solitary waves are shown. It is interesting to note that the speed of the dominant periodic wave decreases with increasing Re_G. While this behavior may be counterintuitive, it is easily explained. As Re_G increases, steady waves have larger

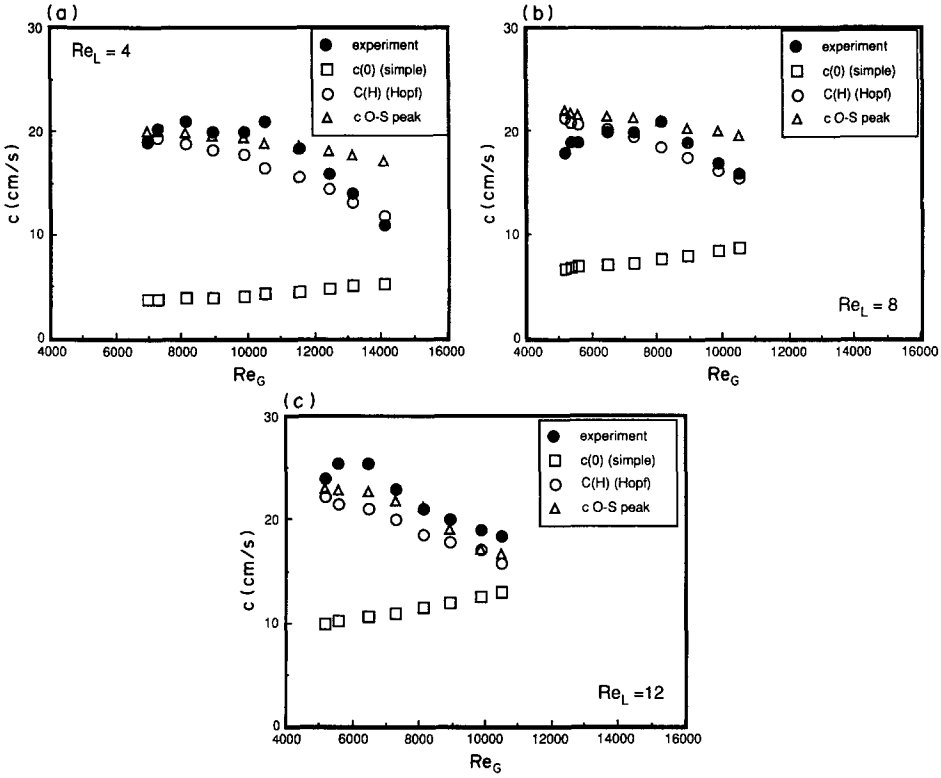

Figure 8. $c - \mathrm{Re}_G$ plots of wave data showing Hopf and simple bifurcation curves.

amplitudes (a result of the greater degree of interfacial stress) and tend to have longer wavelengths as well (probably in an attempt to minimize their interfacial curvature). Because the speed decreases as the wavelength increases, the observed wave speed decreases with increasing gas velocity. Solitary waves are seen to travel much faster than periodic waves and to exist in a region of $c - \mathrm{Re}_G$ parameter space which opens in a direction away from periodic waves. Results for solitary waves on vertical falling films (Chang 1987; Nakoryakov *et al.* 1976), indicate that as the amplitude of solitary waves increases, the speed will as well. This is expected for the present situation however, we have not made these measurements.

4. DISCUSSION

The data presented above suggest that the equation developed by Jurman & McCready (1989), with parameters obtained from Abrams (1984) and Abrams & Hanratty (1985), should accurately describe the behavior which occurs on thin, viscous films which are sheared by a turbulent gas flow.

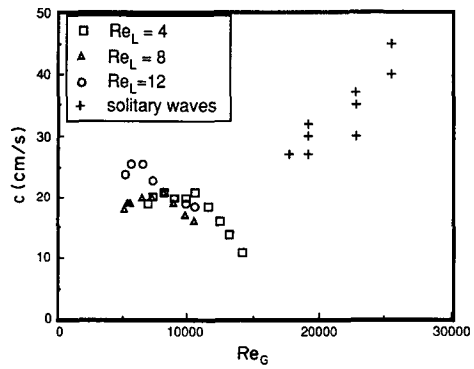

Figure 9. Experimental wave speeds for periodic and solitary waves.

The obvious limitations are its inability to describe regions where the curvature is great or cases where the dominant waves do not have wavelengths significantly longer than the film thickness. The analysis and data presented above demonstrate methods for getting bounds on speeds and wavelengths of periodic waves. Periodic waves are observed in all cases to travel close to but faster than the neutrally stable modes of the Hopf curve. In addition, the Hopf curve serves as a lower bound on the wavenumber of periodic waves. It is expected that numerical solutions of [8] could be done to predict the amplitude of stable periodic waves.

However, several important issues remain unresolved. As mentioned in the introduction, it would be of interest to be able to predict *a priori* the type of waves (i.e. solitary or periodic) which occur for a given set of flow conditions. This could be determined by a normal form analysis coupled with a numerical study of the solutions to [8] similar to that done by Hwang & Chang (1987). While fully-developed solitary waves may have curvatures which exceed the degree of nonlinearity contained in [8], it is quite likely that near the point of transition, [8] will accurately describe their behavior.

A second unresolved issue involves the selection process which governs the wavelength and amplitude of the observed waves. The data indicate that the Hopf curve will serve as a boundary on the periodic waves but the present analysis cannot tell how close the waves will lie. One way of resolving this issue would be to numerically integrate [8] and then test the stability of the solutions by reintroduction of the time derivatives. Presumably, the most stable form will be the one which corresponds to the waves observed experimentally. Integration of [8] can also be done for the region where solitary waves occur. It is expected that this effort would be less fruitful as the observed waves may have curvatures too great for [8] to describe.

Solitary waves exist at $Re_G \gtrsim 11{,}000$. Their occurrence appears to be a function of Re_L as well (a point which could be confirmed by a nonlinear analysis). However, such an analysis would not provide insight into an equally important question with regards to heat and mass transfer, atomization and pressure drop. How many of the waves pass a given location during a given period of time? To resolve this issue (which does not arise, for obvious reasons, with periodic waves), it is necessary to examine the mechanism by which solitary waves are formed. At high Re_G, where

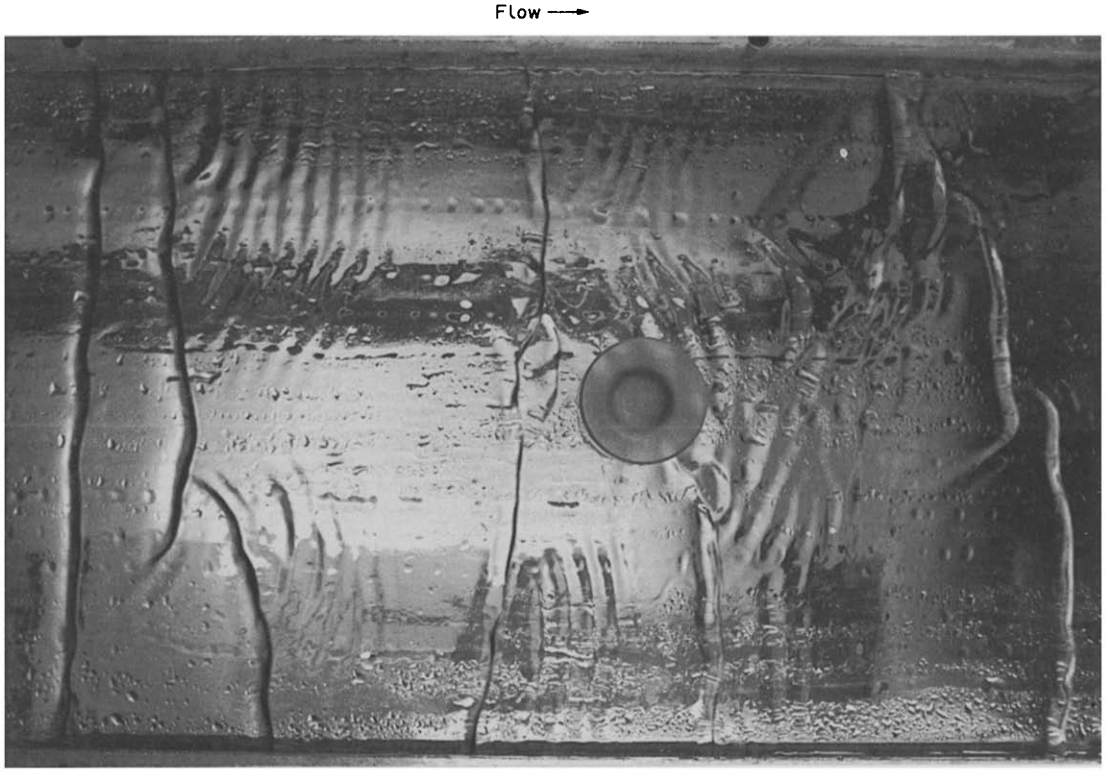

Figure 10. Photograph of flow at $Re_L = 9$ and $Re_G = 13{,}900$. The flow is from left to right.

solitary waves occur, the film is linearly unstable to infinitesimal disturbances, suggesting that periodic waves should also form. Figure 10 shows a photograph of the waves for $Re_G = = 13{,}900$ and $Re_L = 9$. The view is from the bottom of the channel and the flow is from left to right. The dark bands which span large parts of the channel are solitary waves; periodic waves, which for these conditions have shorter spanwise widths, are also seen (any droplets which appear are attached to the top wall). Wave tracings and visual observations indicate that periodic waves are unstable and quickly evolve to another form. In an attempt to determine the exact events which transpire in this regime, we have observed this process with a videocamera and recorder. From figure 10 and the slow motion projection of the videotape, it can be seen that after the passage of a solitary wave, which leaves behind a smooth film, periodic waves form rapidly. These grow until one of two events occur. First, it is possible for one of the new periodic waves to reach an amplitude large enough to become a solitary wave. If this happens, the wave suddenly increases in speed and engulfs any periodic waves in front of it. A second and more likely scenario is the engulfment of all of the newly formed periodic waves by a solitary wave from upstream. In either case, the process begins again. At steady state, it is assumed that the number of solitary waves does not change with time or distance. As some new waves are being created, others must disappear. This process occurs either by faster waves catching slower waves and engulfing them or occasionally by waves appearing to die spontaneously (an event which apparently occurs when the amplitude gets too large).

It is of interest to comment upon the relation between the solitary waves observed in the present study and "roll waves" as observed by Hanratty & Hershman (1961). Hanratty & Hershman (1961) noted that for water as a fluid, a transition from a pebbly surface to roll waves occurs if the Re_L (defined as 4 times the present Re_L) exceeds about 100 when $Re_G \gtrsim 15{,}000$. Andreussi *et al.* (1985) and Miya *et al.* (1971) extended this study to include fluids more viscous than water. Figure 3 of Andreussi *et al.* (1985) indicates that the Re_L at the transition to roll waves decreases smoothly with increasing viscosity. Our present data, which fall on the upper viscosity end of this plot indicate that so-called "roll waves" are the same as solitary waves. (Our observations suggest for fluids as viscous as 15 cP, the waves are probably not breaking.) Bruno & McCready (1988) speculate that for all fluids in the low Re_L region (below $Re_L = 25$), "roll waves" are actually solitary waves; for low viscosity fluids these may begin to break. If this is the case, then a nonlinear analysis of [1] which reveals the entire qualitative structure around the double zero point may explain the transition to roll waves on thin films which has eluded all linear analyses done to date.

Acknowledgements—This work is being supported by the Department of Energy under Grant DE-FG02-88ER13913. The authors would also like to thank Dr H.-C. Chang for helpful discussions about nonlinear analysis.

REFERENCES

ABRAMS, J. 1984 Turbulent flow over small amplitude solid waves. Ph.D. Thesis, Univ. of Illinois, Urbana.

ABRAMS, J. & HANRATTY, T. J. 1985 Relaxation effects observed for turbulent flow over a wavy surface. *J. Fluid Mech.* **151,** 443–455.

ALEKSEENKO, S. V., NAKORYAKOV, V. Y. & POKUSAEV, B. G. 1985 Wave formation on a vertically falling liquid film, *AIChE Jl* **32,** 1446–1460.

ANDREUSSI, P., ASALI, J. C. & HANRATTY, T. J. 1985 Initiation of roll waves in gas–liquid flows. *AIChE Jl* **31,** 119–126.

BARRDAHL, R. 1986 On the stability of falling films—periodic finite-amplitude waves. *AIChE Jl* **32,** 789–797.

BRAUNER, N. & MARON, D. M. 1983 Modeling of wavy flow in inclined thin films. *Chem. Engng Sci.* **38,** 775–788.

BRUNO, K. & MCCREADY, M. J. 1988 Origin of roll waves in gas–liquid flows. *AIChE Jl* **34,** 1431–1440.

CARR, J. 1981 *Applications of Centre Manifold Theory*. Springer, New York.

CHANG, H.-C. 1986a Nonlinear waves on liquid film surface—I. Flooding in a vertical tube. *Chem. Engng Sci.* **42,** 2463–2475.

CHANG, H.-C. 1986b Traveling waves on fluid interfaces: normal form analysis of the Kuramoto–Sivashinsky equation. *Phys. Fluids* **29,** 3142–3147.

CHANG, H.-C. 1987 Evolution of nonlinear waves on vertically falling films—a normal form analysis. *Chem. Engng Sci.* **42,** 515–533.

CHEN, L.-H. & CHANG, H.-C. 1986 Nonlinear waves on liquid film surface—II. Bifurcation analyses of the long-wave equation. *Chem. Engng Sci.* **42,** 2477–2486.

CHU, K. J. & DUKLER, A. E. 1974 Statistical characteristics of thin, wavy films: part II. Studies of the substrate and its wave structure. *AIChE Jl* **20,** 695–706.

COHEN, L. S. & HANRATTY, T. J. 1965 Generation of waves in the concurrent flow of air and a liquid. *AIChE Jl* **11,** 138–144.

CRAIK, A. D. D. 1966 Wing-generated waves in thin liquid films. *J. Fluid Mech.* **26,** 369–392.

FUKANO, T. A., ITOH, A. & OUSAKA, A. 1985 Breakdown of a liquid film flowing concurrently with gas in horizontal line. *PhysicoChem. Hydrodynam.* **6,** 23–47.

GUCKENHEIMER, J. & HOLMES, P. 1983 *Nonlinear Oscillations, Dynamical Systems, and Bifurcations of Vector Fields.* Springer, New York.

HANRATTY, T. J. 1983 Interfacial instabilities caused by air flow. In *Waves on Fluid Interfaces* (Edited by MEYER, R. E.), pp. 221–259. Academic Press, New York.

HANRATTY, T. J. & ENGEN, J. M. 1957 Interaction between a turbulent air stream and a moving water surface. *AIChE Jl* **3,** 299–308.

HANRATTY, T. J. & HERSHMAN, A. 1961 Initiation of roll waves. *AIChE Jl* **7,** 488–497.

HENSTOCK, W. H. 1977 The effect of a cocurrent gas-flow on gas–liquid mass transfer. Ph.D. Thesis, Univ. of Illinois, Urbana.

HENSTOCK, W. H. & HANRATTY, T. J. 1976 The interfacial drag and the height of the wall layer in annular flows. *AIChE Jl* **22,** 990–1001.

HWANG, S.-H. & CHANG, H.-C. 1987 Turbulent and inertial roll waves in inclined film flow. *Phys. Fluids* **30,** 1259–1268.

JURMAN, L. A. & MCCREADY, M. J. 1989 A study of waves on thin liquid films sheared by turbulent gas flows. *Phys. Fluids.* In press.

LIN, S. P. 1974 Finite amplitude side-band instability of a viscous film. *J. Fluid Mech.* **63,** 417–429.

MARON, D. M., BRAUNER, N. & DUKLER, A. 1985 Interfacial structure of thin falling films: piecewise modelling of the waves. *PhysicoChem. Hydrodynam.* **6,** 87–113.

MARTIN, C. J. & AZZOPARDI, B. J. 1985 Waves in vertical annular flow. *PhysicoChem. Hydrodynam.* **6,** 257–265.

MCCREADY, M. J. 1986 Spectral behavior of capillary waves in gas–liquid flows. *Phys. Fluids* **29,** 2836–2842.

MIYA, M., WOODMANSEE, D. E. & HANRATTY, T. J. 1971 A model for roll waves in gas–liquid flows. *Chem. Engng Sci.* **26,** 1915–1923.

NAKAYA, C. 1975 Long waves on a thin fluid layer flowing down an inclined plane. *Phys. Fluids* **18,** 1407–1412,

NAKORYAKOV, V. E., POKUSAEV, B. G. & ALEKSEENKO, S. V. 1976 Stationary two-dimensional rolling waves on a vertical film of fluid. *Inzh-Fiz. Zh.*, **30,** 780–785.

NENCINI, F. & ANDREUSSI, P. 1982 Studies of the behavior of disturbance waves in annular two-phase flow. *Can. J. chem. Engng* **60,** 459–465.

PUMIR, A., MANNEVILLE, P. & POMEAU, Y. 1983 On solitary wave running down an inclined plane. *J. Fluid Mech.* **135,** 27–50.

TELLES, A. S. & DUKLER, A. E. 1970 Statistical characteristics of thin, vertical, wavy, liquid films. *Ind. Engng Chem. Fundam.* **9,** 412–421.

WASDEN, F. K. & DUKLER, A. E. 1987 Insights into the hydrodynamics of free falling wavy films. Presented at *AIChE A. Mtg*, New York, Paper 66D (1987).

WEBB, D. R. & HEWITT, G. F. 1975 Downwards co-current annular flow. *Int. J. Multiphase Flow* **2,** 35–49.